

Development of finger vein phantoms with realistic finger vein patterns

Rasmus van der Grift

Faculty of Electrical Engineering, Mathematics and Computer Science (EEMCS),
Datamanagement & Biometrics (DMB), University of Twente, 7500 AE Enschede, The
Netherlands

September 8, 2021

This report will cover a method to make phantom fingers with realistic finger veins. Just like real blood vessels, these veins can be detected under NIR light. These phantom fingers can help future extraction methods and finger vein scanners with their performance as the position of the veins is known unlike their real counterparts. It turns out that this method can also be used for spoofing as the performance of Miura max curvature together with ICP drops down if phantom fingers are introduced which represent a real finger.

1 INTRODUCTION

Fingerprint or face recognition is increasingly becoming an integral part of personal devices. Another emerging biometric technology is blood vessel based recognition and identification. Advantages of this finger vein pattern based biometric recognition are good resistance to presentation attacks, very low error rates and user convenience comparable to fingerprint recognition [13]. Face and fingerprint recognition systems are often tested and optimized using data with their ground truths. These ground truths are relatively easy to obtain because this information is present on the surface of the body. Since blood vessels are present inside the human tissue, obtaining the ground truth is not as easy. Using various 3D printing techniques, a phantom of a finger can be created where the ground truth is known. This technique can be used to create a data set that can be used to improve finger vein recognition systems in the future.

2 RELATED WORK

This section will discuss the related work used in this research.

2.1 Types of Sensors

There are several types of scanners. The 'handbook of Vascular Biometrics'[13] summarises different types of sensors for finger vein recognition. Because haemoglobin in veins has a higher absorp-

tion of Near-Infrared (NIR) light than the surrounding tissue, the vascular pattern inside a finger can be captured by a device sensitive to NIR light. There are several ways to illuminate the finger to extract blood vessels. The main types found in existing devices are shown in Figure 1.

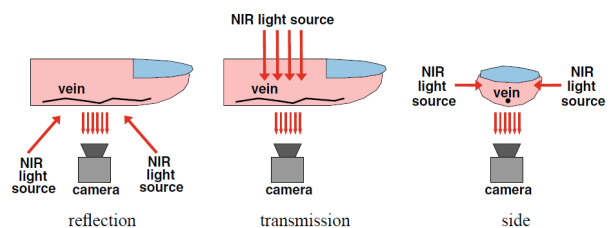


Figure 1: Reflection, transmission and side illumination acquisition.[13]

In the first scanner, the light sources are on the same side as the camera. This allows the device to be more compact. The disadvantage of this method is that the image sensor picks up mainly the reflected light from the surface of the finger, since the light penetrates little into the skin. Therefore, this method provides images with low contrast between tissue and veins. The second finger vein scanner uses light transmission that passes directly through the finger. This provides high contrast images of the vascular patterns because the light passes through the finger and no surface reflections are captured. The disadvantage of this method is that the user has to put their finger into the device in such a way that they cannot see their finger, which can cause discomfort. The last scanner is based on illumination. This method still allows for an open sensing device with reflection, transmission, and side illumination so that the user can see their finger. The light sources are placed on either one side or both sides of the finger. The NIR light passes through the sides of the finger and is scattered there before being captured by the image sensor. This method does provide high contrast images. However, the sides of the finger are overexposed in the images.

2.2 Relation between depth and size of blood vessels

A paper is presented on the use of near infrared light to safely and effectively visualize subsurface blood vessels to facilitate blood sampling in children, showing a study of various sizes of blood vessels at increasing depths. NIR light is able to penetrate deep enough into tissue to visualize blood vessels used for peripheral venous and arterial access due to lower absorption and scattering compared to visible light. Figure 2 shows a sample of the phantom veins at various depths. The reader may notice that the vessels have less contrast on the NIR image when they are smaller in size and/or lay deeper.

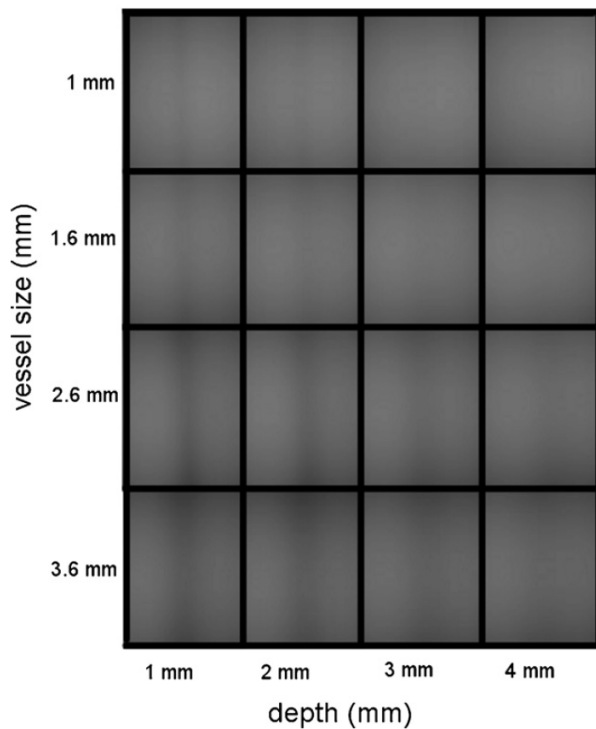


Figure 2: Phantom images of the four different sizes of blood vessels at increasing depth.[3]

2.3 Extraction of Finger-Vein Patterns Using Maximum Curvature Points and ICP

A biometric system for identifying individuals by the pattern of veins in a finger uses the maximum curvature proposed by Miura [8]. Infrared light is used to take an image of a finger showing the vein patterns. These have different widths and brightness levels that change over time due to variations in the amount of blood in the vein depending on temperature, physical conditions,

etc. This method attempts to robustly extract the exact details of the imaged veins and presents a method for computing local maximum curvatures in cross-sectional profiles of a vein image. This method can consistently extract the centerlines of the veins without being affected by the variations in vein width and brightness, making the pattern matching very accurate. Experimental results show that this method extracts patterns when the vein width and brightness fluctuate. Also, the same person identification error rate was 0.0009%, which is much better than that of other conventional methods.

2.3.1 Finger-vein Pattern Recognition Based on ICP on Contours

A complement to this method of maximum curvature is the ICP method[10]. An important step in finger vein recognition is proper alignment of the finger vein patterns. This alignment method is used to deal with variations in finger posture and to increase the stability of finger vein authentication. Figure 3 shows an overlap of two finger vein skeletons.

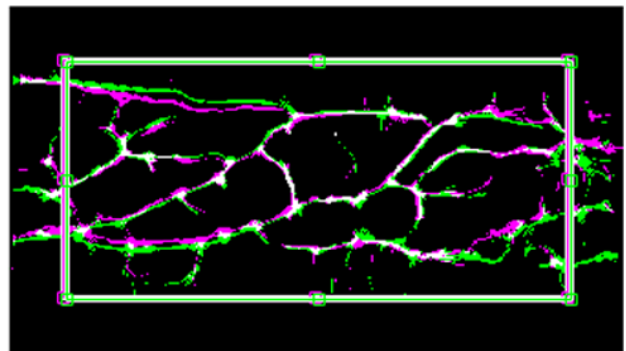


Figure 3: Overlapping of finger veins after using ICP and Maximum curvature [10].

After the alignment process, the method of maximum curvature from the above section is applied. In the research, ICP caused a higher true score, which means that it is a good complement to the method. The experimental results show that the accuracy of the proposed method is improved in the verification case and slightly higher than the state-of-the-art registration method, which is called centerline registration. The use of ICP for registration resulted in a reduction of EER to 0.3% (from 0.7% for centerline registration) and a reduction of FNMR@FMR0.01 to 0.7% (from 2.0% for centerline registration) [10].

3 METHODS

This section discusses a method of making phantom fingers that can be used in future methods of finger vein extraction and finger vein scanners. Figure 4 shows a simple overview of the steps to make the 3D printed phantom fingers.

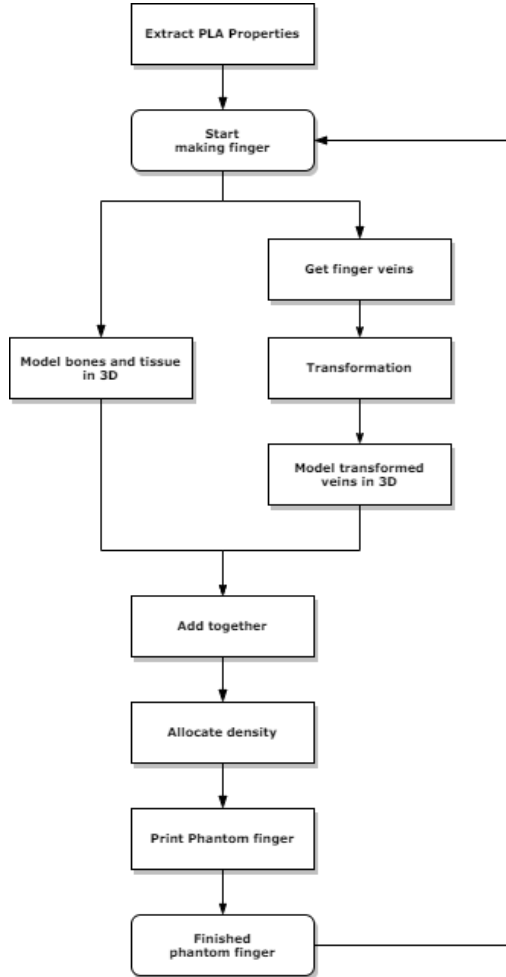


Figure 4: Overview of making phantom fingers

3.1 Determine PLA properties

Since blood, tissue, and bones have different NIR light properties [6], it was proposed to investigate the properties of different colors and densities of polylactic acid (PLA). There are many different brands that produce PLA, and each has several colors to choose from. In this section, methods for extracting different properties of PLA are discussed in case someone wants to create phantom fingers with realistic finger veins.

3.1.1 Density

Real fingers have differences in the thickness of tissue and bones. Most often, the bones are thicker at the head and base, as opposed to their shaft. Thicker parts of the bone usually have less

tissue around them. Bones absorb less NIR light than tissue, resulting in brighter areas in the NIR image of a finger around the head and base of the bones. This phenomenon can be observed in Figure 5.

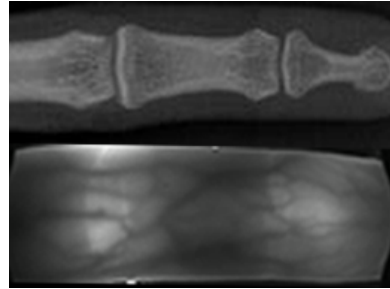


Figure 5: Head and base of a bone has thinner tissue around it that causes lighter areas in the NIR image of a finger [9]

The first method is constructed to see if differences in the density of a 3D model affect the NIR light absorption of PLA. A solid tube is created in Solidworks [12] as shown in Figure 6. Using the slicer software Simplify3D [11], the density is given at different levels.

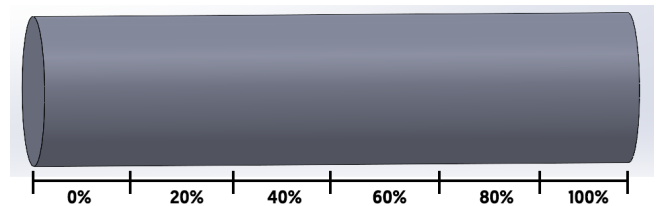


Figure 6: Solid tube with density percentage on different levels.

From Figure 7, it can be concluded that the less dense the tube, the less light it absorbs, resulting in a brighter section of the tube under NIR light. This information can be used to create the same NIR light effect as bones and tissue.

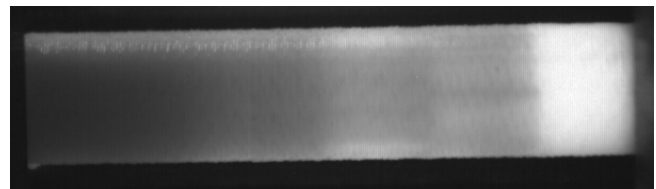


Figure 7: Solid tube made in Solidworks with changing density level done by Simplify3D[11].

3.1.2 Colors

Another property of PLA is its color. In tests, the color was found to have an effect on the ab-

sorption level of NIR light. A solid tube is designed and printed in several different colors of a test set of PLA. The test set used is from Renkforce [2] (item no.: 1531460). Since the material and color can vary from manufacturer to manufacturer, the reader should keep in mind that the NIR light properties of the colors are not the same for every manufacturer and may be different for their particular PLA. Figure 8 shows the Solidworks model of a tube that will have a difference in density on every centimeter of the tube. The density will change from 100% infill to 0% infill. Two smaller tubes in the color gray with a diameter of 1.0mm with 100% infill will be added inside the large tube to mimic vessels and to see how the vessels behave under different NIR light situations. It is important to note that the 3D printer must have two extruders. Otherwise, it is not possible to print two different PLA materials at the same time.



Figure 8: Solid tube with two straight imitation vessels made in Solidworks.

Figure 9 shows all the colors from the test set. Each color is irradiated with different strengths of NIR light and compared to a real finger.



Figure 9: 3D printed colored tubes.

Figure 10 shows all the different colored tubes under different strengths of NIR light. As can be

seen in the figure, red, purple, orange and yellow absorb less NIR light than finger tissue. Green, blue and white show similar NIR light absorption behavior as finger tissue. Brown, gold, and gray absorb more NIR light than finger tissue. Blood absorbs more NIR light than finger tissue due to hemoglobin. Therefore Brown, gold and gray can be used for blood vessels in the finger. Depending on the diameter of the resulting phantom finger, the density should be chosen to mimic the NIR levels of a real finger.

3.1.3 Depth of vessels

As can be seen in section 2.2 depth of the blood vessels affects the contrast and sharpness of the fine details. Even in real fingers, the blood vessels are at different depths within the finger. In this section, we discuss a way to recreate and observe different depths of fake blood vessels printed with Renkforce PLA. Figure 11 shows a Solidworks model of a tube with replicated vessels at different depths within the tube. A hollow inside of the tube was chosen so that the tissue would have a higher contrast to the vessels in the NIR light spectrum.

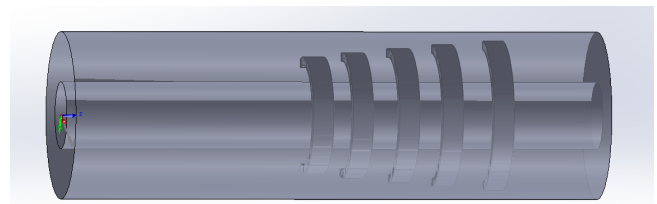


Figure 11: Solidworks model of a tube with fake vessels on different level of depths.

Figure 12 shows the NIR image of the model from Figure 11. The reader can see that the closer the imitated vessel is to the surface, the sharper it is. It can also be seen that deeper vessels have less contrast with the surrounding skin tissue.

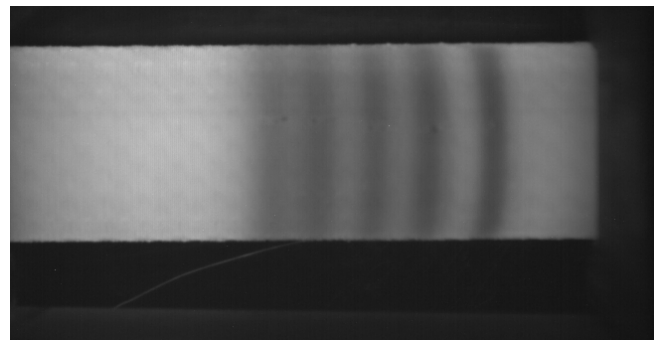


Figure 12: NIR image of the 3D printed model from Figure 11.

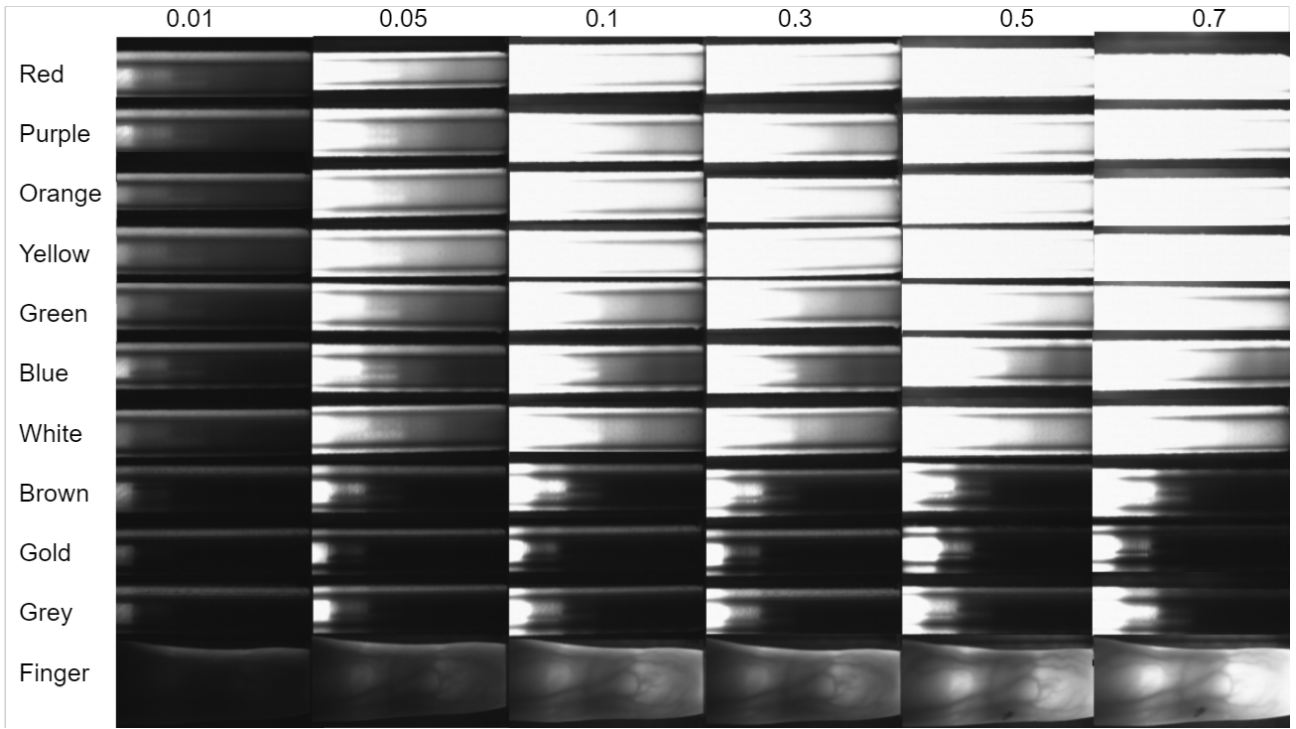


Figure 10: Renkforce[2] PLA colored tubes under different NIR light levels.

3.2 Extract finger and vein properties

In this section, a method for extracting features from fingers is discussed. Using this method, finger vein skeletons can be generated and used to produce phantom fingers. In this work, NIR light images of real fingers are used along with a finger vein extraction method to obtain the skeletons that are printed into the finger phantoms.

3.2.1 Bones and tissue

Skin tissue absorbs more NIR light than bones [6]. Figure 10 shows that the density of real fingers causes a different contrast in NIR images, which can be mimicked by different densities in PLA. The tissue is modeled as a tube that holds the bones and blood vessels. The bones have different sizes and shapes. In this, the bones are modeled with multiple cylinders stacked on top of each other, each with a different diameter. Once the bones are placed in the "tissue" tube, the bones must be extracted from the solid tube using Solidworks' cavity feature. Otherwise the slicer will think 2 parts have to be printed in the same spot. Figure 13 shows the model of the "tissue" tube with the bones inside. Because the printer has only 2 extruders, the bones are made with the same color as the tissue but with a lower density to still mimic the behaviour of real tissue and bones. With the slicer software simplify3D it is possible

to give different densities to different parts of a model. To replicate the real situation, a higher density is chosen for the tissue than for the bones. The distance between the bones and the surface leads to different NIR absorption levels that can be observed under NIR light, which is shown in Figure 14.

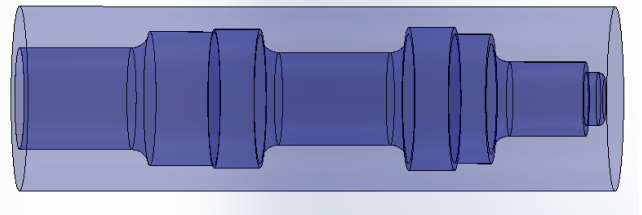


Figure 13: Solid tube with the bone structure inside.

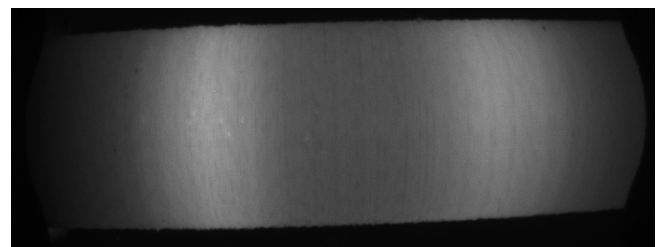


Figure 14: Tissue and bone imitation under NIR light.

3.2.2 Finger vein extraction

Finger vein skeletons have to be printed within the finger. This paper is about a skeleton extracted from a 2D NIR image and then processed into a 3D skeleton model. The 2D image of the finger is analyzed and a skeleton is created using Miura Maximum curvature [8]. Since this method produces a skeleton that does not represent the width of the veins, the thickness must also be considered. The thickness of the vessels is determined by placing the binary image of the skeleton on the NIR image and looking at the pixel values in the area around it. On a NIR image, a vein is darker than the surrounding tissue because of its hemoglobin [6]. A pixel is assigned as a vessel if the pixel value is within σ of the minimum value of the local area. Figure 15 shows an example of a local range of pixel values.

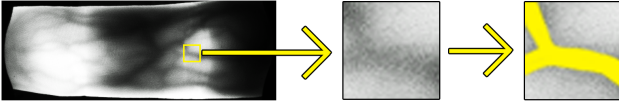


Figure 15: thickness based on local area

Another challenge occurs when the algorithm detects finger veins which are not there. First, contrast differences present at the joints of bones can cause the algorithm to identify these transitions as veins. Another reason could be the sigma of the Miura algorithm which determines the derivatives of the algorithm. If this sigma is too low it will be more sensitive to smaller veins or distortions. These detected veins have to be filtered out. The proposed method in this thesis is to again look at the local area around the skeleton and concluding there isn't enough contrast. If there isn't enough contrast within the local area the algorithm will declassify the detected vein. Also tweaks by hand are an option if spoofing is the intention.

3.3 3D print preparation

Now that the skeleton of the veins has been determined, the veins must be converted into a 3D model. Since the initial image is 2D, a rotational transformation must be performed. Since a tube is used as a finger, the transformation is relatively simple. Figure 16 shows an overview of how the transformation works. It shows a finger a finger vein located within the finger at an unknown depth. This blood vessel is projected onto a 2D image that does not have the 3D information of

the vessels. For a finger phantom, this 2D image can be wrapped in the tissue around a tube. Using the radius (r) of the finger and the displacement (d) of a vessel from the center, the angle (σ) between two points on the surface can be calculated using the equation 1. The arc (a) at the surface can be calculated using the radius and angle using the equation 2 to estimate the width of the vein and the distance to the center.

$$\sigma = \arcsin\left(\frac{|d|}{r}\right) \quad (1)$$

$$a = \sigma * r \quad (2)$$

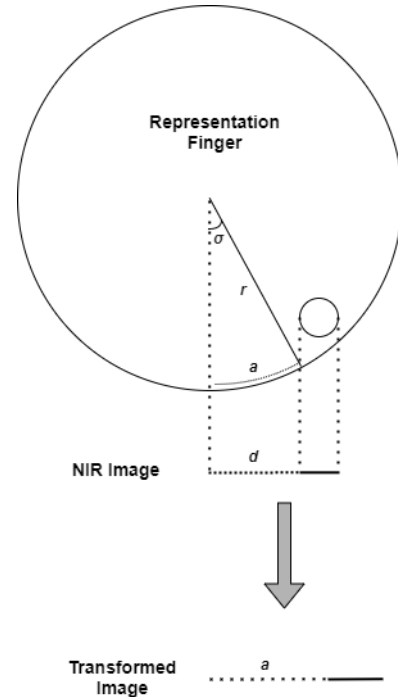


Figure 16: Transformation.

Figure 17 shows the result of an example before and after.



Figure 17: Result of the transformation before and after.

The replica of the vessels is now ready to become 3D. To import the images of the vessels into Solidworks, they need to be transformed into sketches. A Drawing Exchange Format (.DXF) file was developed by Autodesk [5] as a sort of universal format for storing CAD models. The DXF files can be imported into Solidworks as sketches. There are several online image \rightarrow DXF converters. For this research, a standalone program is created using the Python library ezdxf [7]. First, the `findContours()` function of OpenCV [1] is used to find the contours with their child contours in the corresponding hierarchy. These contours are used for the line segments of the DXF file. This file can be exported and used as a sketch in Solidworks. To get the correct dimensions for the phantom veins, a calibration tool can be created. This is done by printing a square with known dimensions and taking a NIR image of it with a finger on top. This helps in resizing the model to the correct size. Figure 18 shows a finger with a 3D printed square to get the correct size of the finger veins.

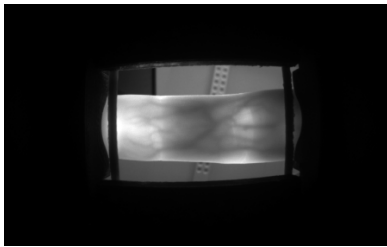


Figure 18: Finger with a 3D printed square to calibrate the size of the model

Once the veins have been imported into Solidworks as sketches, they are inserted into the finger phantoms. This involves using a smaller tube than the outside of the finger so that the veins are inside the finger phantom. The veins are given a depth of $0.8mm$ because the extruders can only print in layers of $0.4mm$ which on it self was not enough to get the desired effect. The smaller tube is removed so that only the veins are visible. Just like the bones in section 3.2.1, the veins must be extracted from the tissue so that they do not overlap during the printing process.

3.4 Model of a phantom finger with realistic finger veins

With all the above information, a Solidworks model of a phantom finger with realistic finger veins can be created.

The model consists of 3 main parts:

1. Tissue

2. Bones
3. Blood vessels

Each part can consist of several smaller parts, but in this research, each main part consists of one Solidworks model. These models can be exported to Standard Triangle Language(STL) files. These STL files can be imported into a slicer such as Simplify3D [11], which then controls the 3D printer. Figure 19 shows a Solidworks model of a phantom finger with realistic finger veins on one side of the finger.

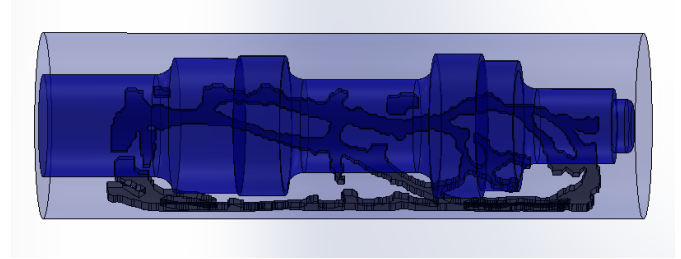


Figure 19: Solidworks model of phantom finger with realistic finger veins.

3.5 Data set

Now that a concept for creating phantom fingers is proposed, a data set can be created. Since the ground truth of each phantom finger in the dataset is known, they can be used to test finger vein systems more reliably than if real fingers were used. To future-proof the dataset, several pieces of information must be stored. A list is shown below:

- STL (and point cloud XYZ) of the vessel structure
- STL of the tissue/bone part
- 2D Input image
- 2D Output images (different angles)

The performance of a matching algorithm can be observed by comparing all images in a database. Assuming that there are multiple images of the same finger, a histogram of genuine and imposter scores can be constructed. A genuine score is based on two images of the same finger. An imposter score is based on two images of different fingers. An example of such a histogram is shown in Figure 20. This figure shows an algorithm based on Miura [8] maximum curvature with ICP [10]. A small data set is used to illustrate that genuine fingers have a higher match rate than those of impostors. The small dataset is created by using eight fingers with five photos of each finger. The algorithm knows which finger is in the image and

can determine genuine and imposter matches. A data set which is created using the phantom fingers should have similar behavior to the real data set.

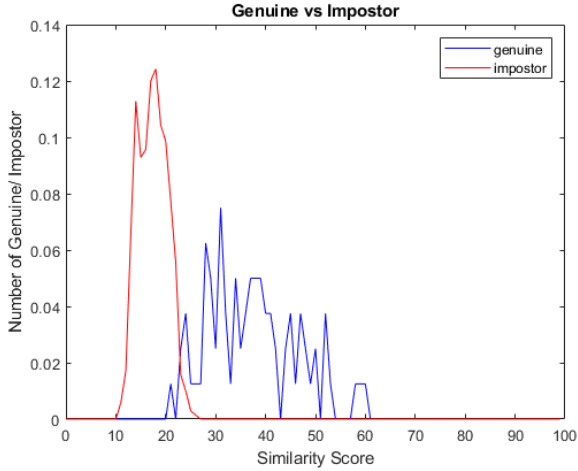


Figure 20: Match rate of a small data set with real fingers.

3.5.1 Spoofing

Phantom fingers in this research are made using images of real fingers. These phantom fingers can be compared to the original images to see if it is possible to spoof real fingers and fool the vein recognizer. The finger vein patterns of the real and phantom fingers are extracted using the maximum curvature, as shown in section 2.3. To align the fingers properly, ICP is used as described in section 2.3.1. A new data set can be constructed by combining a dataset of real fingers and a dataset of phantom fingers which are based on these real fingers. The phantom fingers are assigned differently to their real counterpart and will count towards the imposter score.

4 EXPERIMENTAL RESULTS AND DISCUSSION

This section discusses the results obtained by combining all the methods described in section 3.

4.1 Setup

The laboratory where the experiments are performed has several finger vein scanners. A scanner built by T. van Zonneveld which is inspired from section 2.1 is used to make the NIR images which are used to extract (phantom) finger veins and compare them to each other.

4.2 Finger phantoms

Figure 19 shows an example of a Solidworks model of a phantom finger to be printed. For the phantom fingers that will be printed in this work, the green and gray Renkforce[2] PLA from section 3.1.2 is used. Green PLA for the tissue and bones and gray PLA for the blood vessels. Since a large filament roll of blue and white was not in stock, green was the next best option for the tissue and bone imitation. Through trial and error, gray was chosen over gold and brown because it gave the closest contrast to real blood vessels and tissue. To match the size of the fake vessel to the real vessel, a small square with an inner surface area of $50mm$ was 3D printed. This square can also be seen when the vessel is imported into Solidworks as a DXF file. Using this technique, it was possible to obtain the ratio that the vessel had to be reduced in size to be the same size as the real counterpart. The phantom veins had to be reduced in size by a factor of 0.24.

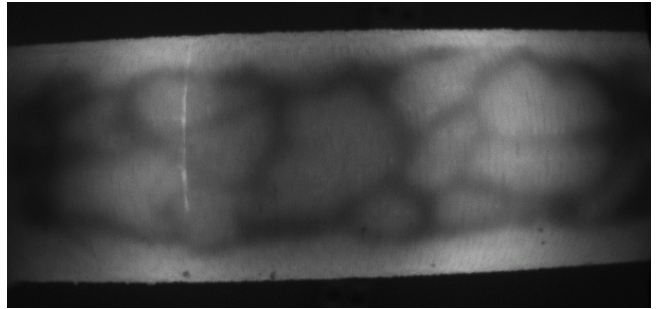


Figure 21: NIR image of a phantom finger.

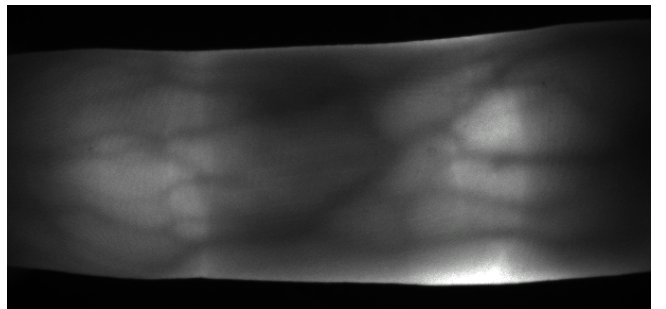


Figure 22: NIR image of a real finger.

Figure 21 shows the NIR image of a phantom finger created using the proposed concept. Compared to the NIR image of a real finger from Figure 22, a few things can be said. First, it is clear that the phantom finger is a tube where the diameter remains the same throughout the finger. The real finger has a more natural appearance with changing diameter along the finger. Another phenomenon that can be observed is the absence of

some finger nerves. Some of them are missing because the 3D printer has a nozzle with a diameter of $0.4mm$. This causes the print to have layers at least $0.4mm$ thick, while the blood vessels can be smaller than that. The sides of the phantom fingers are also lighter than the sides of the real finger. This is partly because blood vessels run all around a real finger, while this phantom finger has no veins on the sides and back.

4.2.1 Double sided phantoms

Real fingers have blood vessels all around the finger. NIR images of real fingers as in Figure 22 show a darker outside of the finger. To mimic this behaviour, a finger phantom is created with finger veins on both sides. Figure 23 and Figure 24 show a phantom finger with single-sided veins and a phantom finger with double-sided veins under the same NIR light. The reader may notice that the phantom finger with double-sided veins absorbs more NIR light, resulting in a darker NIR image. If in the future double-sided finger veins will be printed, it could be that the density of the surrounding phantom tissue has to be lower.

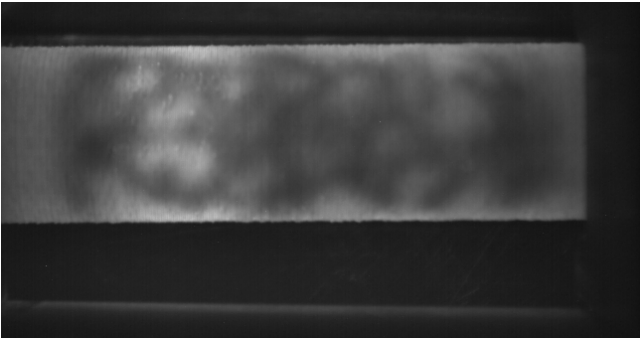


Figure 23: Phantom finger with veins on only one side of the tube.

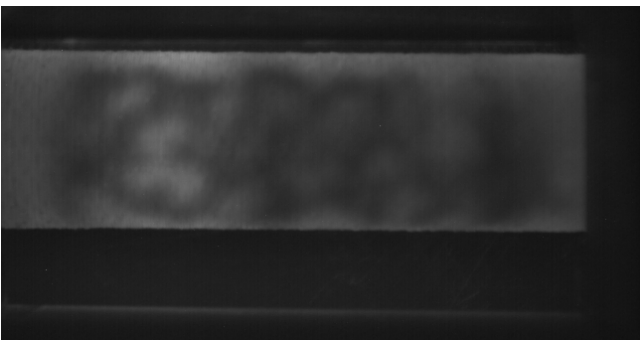


Figure 24: Phantom finger with veins on both sides of the tube.

4.2.2 Performance of Miura and ICP on the phantom finger data set

A small data set of six phantom fingers is created. Five images of each phantom finger are taken with different placement and angles within 10 degrees of the center. This results in a small data set of 30 images. When matching all the images against each other using Miura Maximum curvature [8] and ICP [10], it can be seen that the algorithm can make a clear difference between genuine phantom fingers and the imposter phantom fingers, which can be seen in Figure 25. The reader may notice the similarities between the Figure 20 and 25, with a remark that the match rate of genuine phantom fingers is higher than that of genuine real fingers. Nevertheless, the algorithm can make a clear distinction between the genuine matches and the imposter matches, which gives the impression that Miura and ICP work relatively well with this data set.

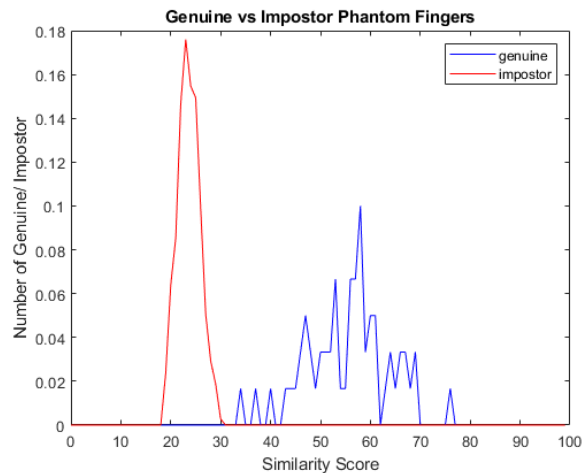


Figure 25: Match rate of a small data set with phantom fingers.

4.2.3 Spoofing

Another challenge was to see if a phantom finger could be created that would outsmart the finger vein algorithms. Two data sets have already been created, one containing NIR images of real fingers and the other containing NIR images of phantom fingers. Since the phantom fingers mimic the real fingers but are not the same fingers in real life, they are assigned as impostor fingers to test the Miura and ICP algorithm. Figure 26 shows that there is more overlap between genuine and impostor scores. Considering Figure 20 and Figure 25, the overlap in the combined dataset is caused by the phantom fingers based on the real fingers, resulting in a higher impostor match score.

This overlap causes low performance of the Miura and ICP algorithm when a low false match rate is desired. Where previously the imposters had a match score of around 20%, now there are many more imposters with a higher match rate of 40%. This phenomenon is mainly caused by the algorithm which is based on matching the extracted finger veins by comparing the skeletons. For the Miura and ICP algorithm, it does not matter if it looks like a finger in the NIR image, but rather if the extracted phantom veins are similar to the extracted veins of the real finger. Matching algorithms which are also based on NIR images or that take into account the vividness of the finger are likely to do much better recognizing the spoof attempts of these phantom fingers.

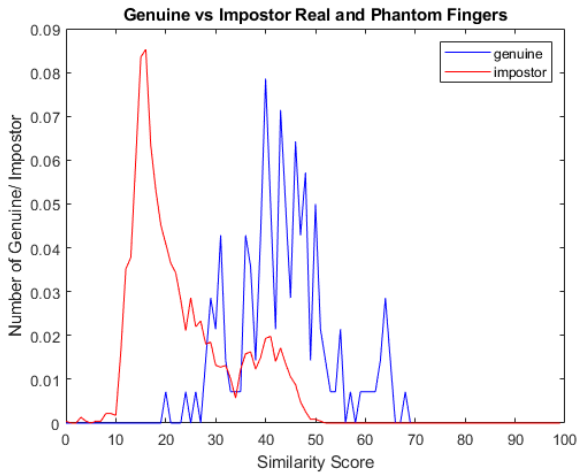


Figure 26: Match rate of a small data set with real and phantom fingers combined.

One thing that has been noted is that NIR images of fingers of each person differ. Everyone has different fingers with different densities and veins at different depths. This sometimes leads to difficulty in extracting the finger vein pattern. This may be a malfunction on the part of the scanner, but some individuals have had fingers with low contrast between the veins and tissue, resulting in an empty vein extraction.

4.3 3D printer experience

If someone were to attempt to replicate these phantom fingers, it might be useful to have a description of some of the challenges that had to be overcome during the process of printing the phantom fingers. Since the printer in the lab is mainly intended for prototyping, it is not suitable for precise work. The nozzles are 0.4 mm, which affects the smaller phantom blood vessels of the model. Another problem occurred when

the printer bed was not correctly calibrated. This caused the print to fall over due to extruders hanging low or PLA being placed incorrectly because the extruders were too high. The last problem was the stickiness of the print bed. If it wasn't sticky enough, the phantom finger would fall over and the print would fail.

5 FUTURE WORK

Although this work shows a promising way to produce phantom fingers that can even be used to spoof certain finger-vein matching algorithms, there is still room for improvement.

5.1 Larger data set

First of all, the results in this research are based on small data sets consisting of a few fingers. To get more reliable results, a larger data set with more real fingers and more phantom fingers must be created.

5.2 Realistic look of the phantom finger

Another thing that can be improved is the appearance of a phantom finger in real life and on the NIR image. Physically, the finger is green and can easily be recognised as a fake finger. PLA with the desired skin color can probably be made with the same properties as the green, blue, and white PLA tested in section 3.1.2. Dye or silicone could also be used but this will have an impact on the NIR properties of the finger.

Also, the shape of the finger can be made to more resemble a real finger. One idea is to extract the outside of the finger, which will give a rough estimate of the appearance of the finger. However, this extraction is still done from 2D images and the intersection of a finger is not a perfect circle. Probably the best way at the time of writing this paper is to scan the finger with a 3D scanner to get the entire external shape of a finger. Also 3D x-ray images can be used to get the shape of the bones inside the finger. The problem that then arises is that the veins are still unknown. One way to solve this is to use a finger vein scanner with multiple cameras so that a 3D point cloud of the veins can be obtained, which can then be inserted into the 3D model of the finger. Since these 3D finger vein scanners are still in their early stages, phantom fingers, as proposed in this work, can help in calibrating these scanners.

5.3 Randomized finger veins

In this work, phantom vessels are created by extracting veins from real fingers. In the future, random vessels could be generated to further expand the data set. There are several ways to do this, one way is described in the paper 'Generating and Analyzing Synthetic Finger Vein Images' [4].

5.4 Printer

Smaller nozzles with a size of for example $0.2mm$ can be used to create even smaller veins within the finger. The printing process will take longer, but the results will be better with more smaller details within the phantom finger.

6 CONCLUSION

This paper has presented a first attempt at developing finger phantoms. There are a few things to keep in mind when creating these finger phantoms. First of all, it is very important to know what material the phantom fingers will be made of. The material should behave similarly to real fingers under NIR light. With the right material and the use of different densities, replicating the behavior of real fingers under NIR light is achieved. In addition, phantom blood vessels can be made by using Miura's maximum curvature to extract the veins. However, in the future, a randomized vein generation method will work faster for a larger dataset. Using the small data sets created in this work, Miura with ICP is tested for its performance. It is found that the maximum curvature of Miura works well together with ICP on datasets without intentional spoofing. Problems occur when there are impostors who want to spoof fingers. The performance of the matching algorithm becomes significantly worse when a low false matching rate is desired. Nevertheless, this work describes a way to successfully create phantom fingers and shows that spoofed fingers can be made to deceive matching algorithms that depend only on the extracted veins and do not look at the NIR images during matching.

7 ACKNOWLEDGEMENTS

I would like to express my sincere thanks to Luuk Spreeuwiers for participating in useful discussions and providing necessary advice and guidance during this research. I would also like to express my special thanks to Geert-Jan Laanstra who helped me a lot in the laboratory during the experimental part of this work. Furthermore, I

would like to thank Pesi Normakristagaluh for the helpful information he provided, Thomas van Zonneveld for participating in discussions and for the use of the NIR image scanner, and finally Dennis Mulder for the tips in modelling in Solidworks and improving the performance of the 3D printer.

References

- [1] G. Bradski. The OpenCV Library. *Dr. Dobb's Journal of Software Tools*, 2000.
- [2] Conrad. Renkforce products. <https://www.conrad.nl>.
- [3] N. Cupera, J. H. Klaessens, J. E. Jaspers, R. de Roode, H. J. Noordmans, J. C. de Graaff, and R. M. Verdaasdonkc. The use of near-infrared light for safe and effective visualization of subsurface blood vessels to facilitate blood withdrawal in children. 2013.
- [4] F. Hillerström, A. Kumar, and R. Veldhuis. Generating and Analyzing Synthetic Finger Vein Images.
- [5] A. Inventor. Autodesk version 22.0. <https://autodesk.com/>, 2018.
- [6] T. C. Z. Julia L. Sandell. A review of in-vivo optical properties of human tissues and its impact on PDT. 2011.
- [7] M. Manfred. Ezdxf, a python package to create and modify dxf drawings, independent of the dxf version. <https://github.com/mozman/ezdxf/blob/stable/docs/source/introduction.rst>.
- [8] N. Miura, A. Nagasaka, and T. Miyatake. Extraction of finger-vein patterns using maximum curvature points in image profiles. 2005.
- [9] A. Murphy and A. Shetty. Finger (pa view). <https://radiopaedia.org/articles/finger-pa-view-2>.
- [10] P. Normakristagaluh, L. Spreeuwiers, and R. Veldhuis. Finger-vein Pattern Recognition Based on ICP on Contours. 2019.
- [11] Simplify3D. Simplify3d slicer software. <https://www.simplify3d.com>.
- [12] D. Systems. Solidworks. <https://www.solidworks.com/>.
- [13] A. Uhl, C. Busch, S. Marcel, and R. Veldhuis. Handbook of vascular biometrics. 2020.